Report Documentation Page

1. Agency Use Only (Leave Blank)	2. Report Date	3. Report Type and Dates Covered
	Dec. 20, 1994	Interim Technical

4. Title and Subtitle
Boron-induced Reconstructions of Si(001) investigated by Scanning Tunneling Microscopy

5. Funding Numbers
N00014-91-J-1629
R&T Code 413S001

6. Author(s)
Yajun Wang and Robert J. Hamers

7. Performing Organization Name(s) and Address(es)
University of Wisconsin-Madison
Dept. of Chemistry
1101 University Avenue
Madison, WI 53706

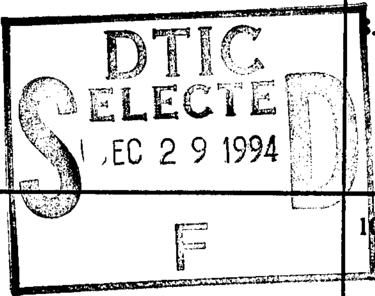

8. Performing Organization Reprt Number
#23

9. Sponsoring/Monitoring Agency Name(s) and Address(es)
U.S. Office of Naval Research
Solid State and Surface Chemistry Program
1101 N. Quincy St.
Arlington, VA 22217-5660

10. Sponsoring/Monitoring Agency Report Number

11. Supplementary Notes
Prepared for publication in Journal of Vacuum Science and Technology A

12a. Distribution/Availability Statement
Approved for public release; distribution unlimited

19941227 013

13. Abstract (Maximum 200 words)

The local geometric and electronic structures of boron-induced reconstructions produced by thermal decomposition of diborane and decaborane on Si(001) has been investigated using scanning tunneling microscopy. STM images show that boron induces several related reconstructions, arising from ordered arrangements of simple structural subunits. These boron-induced atomic rearrangements order even at very low boron exposures, leading to a striking spatial segregation of boron on the surface. Similar reconstructions are observed using diborane and decaborane as boron precursors. Annealing at 1000 Kelvin for 90 seconds substantially improves the surface ordering, without significant diffusion of boron from the surface to the bulk

14. Subject Terms	15.. Number of Pages 24
	16. Price Code

17. Security Classification of Report	18. Security Classification of this Page	19. Security Classification of Abstract	20. Limitation of Abstract
Unclassified	Unclassified	Unclassified	UL

U.S. OFFICE OF NAVAL RESEARCH

GRANT N00014-91-J-1629

R&T Code 413S001

Technical Report #23

Boron-induced Reconstructions of Si(001) Investigated by Scanning Tunneling Microscopy

by

Y. Wang and R.J. Hamers

Accesion For
NTIS CRA&I ☑
DTIC TAB ☐
Unannounced ☐
Justification
By
Distribution /
Availability Codes
Avail and / or Special
A-1

Prepared for Publication

in

Journal of Vacuum Science and Technology

Dec. 20, 1994

Department of Chemistry
University of Wisconsin-Madison
Madison, WI 53706

Reproduction in whole or in part is permitted for any purpose of the United States Government.

This document has been approved for public release and sale: its distribution is unlimited.

Boron-induced Reconstructions of Si(001) Investigated by Scanning Tunneling Microscopy

Yajun Wang and Robert J. Hamers

Department of Chemistry

University of Wisconsin

Madison, WI 53706

Abstract

The local geometric and electronic structures of boron-induced reconstructions produced by thermal decomposition of diborane and decaborane on Si(001) has been investigated using scanning tunneling microscopy. STM images show that boron induces several related reconstructions, arising from ordered arrangements of simple structural subunits. These boron-induced atomic rearrangements order even at very low boron exposures, leading to a striking spatial segregation of boron on the surface. Similar reconstructions are observed using diborane and decaborane as boron precursors. Annealing at 1000 Kelvin for 90 seconds substantially improves the surface ordering, without significant diffusion of boron from the surface to the bulk.

Introduction

Boron is by far the most widely-utilized dopant used in the fabrication of silicon-based semiconductor devices. In chemical vapor deposition (CVD) processes boron is usually introduced through the decomposition of diborane (B_2H_6),[1,2] while in molecular beam epitaxy (MBE) it is introduced using elemental boron[3,4] or boric acid (HBO_2, or anhydrous H_3BO_3).[5-10] In the CVD process, boron affects not only the semiconductor doping, but also affects the epitaxial growth rate of silicon[11,12] and Si:Ge alloys [13] and the surface morphology of the resulting thin films.[14] Recent studies have shown that it is possible to prepare boron-doped layers in which the local boron concentration exceeds the bulk solubility limit by several orders of magnitude.[2] For fabrication of nanoscale electronic devices, the ability to prepare such kinetically-controlled structures represents an important advance in which the random dopant statistics is replaced with atomic-level control.

Despite its widespread use as a p-type dopant, the interaction of boron with Si(001) has only been studied recently. Yu, et al. showed that the reactivity of Si(001) toward B_2H_6 is very low both at 300 Kelvin and at 873 Kelvin. At the higher temperature, decomposition of diborane does produce an electrically-active, boron-doped surface layer[1]. The surface structure and electric properties of the so-called "delta-doped" boron layers on Si(001) have been extensively investigated by Feldman and co-workers.[6-10] These studies confirmed that the boron atoms at the surface are electrically active (implying a

substitutional location), with a coverage of 0.5 monolayer. Electron diffraction studies also showed that the boron-doped surface retained the (2x1) electron diffraction pattern characteristic of the clean surface.[6, 9] A boron coverage of 0.5 monolayers has also been reported using decaborane ($B_{10}H_{14}$) as a precursor. [15]

While scanning tunneling microscopy has previously been used to study boron-induced reconstructions on Si(111)[16, 17], our own recent studies are the first investigations of boron interacting with the more technologically-important Si(001) surface. In our previous work, [18, 19] we showed that decomposition of diborane (B_2H_6) at elevated temperatures on Si(001) produces several ordered reconstructions in which boron atoms occupy substitutional sites, reconstructing the Si(001) surface into small regions with c(4X4) and (4X4) local symmetry. We have previously characterized the localized electrical activity using atomically-resolved tunneling spectroscopy and STM-based photovoltaic measurements, and established the boron coverage within these reconstructions at 1/2 monolayer based on quantitative Auger electron spectroscopy measurements. In this paper, we describe in more detail the nucleation and growth of the boron-induced structures, and we compare growth using both diborane (B_2H_6) and decaborane ($B_{10}H_{14}$).

Experimental

STM experiments were performed in an ultrahigh vacuum (UHV) chamber with a base pressure of less than 10^{-10} torr. Our STM consists of a single-tube scanner mounted at the end of a Burleigh "Inchworm". All feedback and inchworm control electronics[20] were made in-house. The microscope hangs from springs inside an ultrahigh vacuum chamber equipped with a load-lock for exchanging both samples and tips. To avoid sample contamination, no thermocouple or other materials containing transition metals other than molybdenum or tantalum were allowed near the sample at any time. Samples were resistively heated on a separate heating stage by passing DC current through the sample. Temperatures were measured using a calibrated optical pyrometer.

Clean Si(001)-(2x1) surfaces were prepared using n-type (Sb-doped) Si(001) wafers oriented to within 0.25^{o} (Wacker Chemitronic); these were degassed for 12 hours at 900 K, then heated to 1400K for several seconds while maintaining the chamber pressure in the mid 10^{-10} torr pressure range.[21]. After characterizing these surfaces with the STM, they were exposed to either 1% B_2H_6 in He (Liquid Carbonic) or vapor from solid $B_{10}H_{14}$ (Aldrich) through a precision leak valve. Coverages were controlled by varying the pressure and exposure time; all exposures stated in this paper have been corrected for the He dilution and refer to actual exposures of diborane. The purities of B_2H_6 and $B_{10}H_{14}$ were checked with in-situ mass spectroscopy and were identical to previous reports for high-purity samples.[22] Because boron accumulates in the near-surface region, Si(001) samples typically were used for only one experiment before being replaced with a fresh sample.

Results

Fig. 1a shows an STM image of a Si(001) surface which was exposed to 125 L of diborane at 800K. Compared with images acquired prior to exposure, two main changes are observed. The most noticeable change is the appearance of protrusions, several of which are indicated by arrows in fig. 1a. The second change is an increase in the number of localized "dark" regions on the surface, where the apparent height is lower than the average surface height. Control experiments show that these defects disappear after annealing to 1300 Kelvin and arise from the chemical interaction of diborane with Si(001), as will be discussed in more detail. Since the sample temperature used here is above the temperatures required to decompose B_2H_6[1] and to desorb hydrogen[1, 23], these changes can be attributed solely to the effects of boron on the surface.

The structural changes induced by B_2H_6 exposure can be seen more clearly in high-resolution STM images, as in fig. 1b. At this resolution, it can be seen that each boron-induced surface feature actually consists of two protrusions. We will refer to the boron-induced feature consisting of two protrusions as the "A" surface feature. From detailed high-resolution images of the "A" features, we can establish the locations of the individual protrusions with respect to the underlying Si(001) lattice. The local symmetry of the "A" surface features is shown in fig. 1c. In addition, fig. 1c shows quantitative height profile measurements across the top of two "A" units along the <110> direction, showing that the individual protrusions within each "A" feature are separated by 5.4 Å and appear 0.89±0.12Å above the substrate, separated by a trough 0.2 Å deep.

It is striking that even at very low boron exposure, as in fig. 1a and 1b, the boron-induced "A" features already tend to form small ordered regions with local c(4x4) symmetry. The local ordering of the boron-induced "A" features can be seen more clearly after exposing the surface to more diborane. Figure 2 shows STM images of Si(001) surfaces obtained after exposing Si(001) surfaces to 375 Langmuirs B_2H_6 at a surface temperature of 800 Kelvin. In fig. 2a, the boron-induced "A" features show more extensive ordering into small domains of c(4x4) symmetry. For consistency with our previous work, we will refer to this particular structure of c(4x4) symmetry as the β-c(4X4) structure.[18, 19] At this higher coverage, a second change is the appearance of a new surface feature, labeled "B" in fig. 2a and 2b. The "B" features are higher than the "A" features, with an apparent height of 1.3 Å above the underlying Si(001) plane. The "B" features have a bean-like shape with the center of symmetry lying in the center of the dimer row and between two dimers along one dimer row and have a shape and apparent height identical to individual epitaxial Si dimers.[24] These "B" features appear to incorporate into the c(4x4) structure formed from the "A" features; this in turn produces a new ordered structure containing both "A" and "B" subunits, which can be seen to form a more extensive ordered region near the step edge at the right of fig. 2c. This ordered structure again has c(4x4) symmetry but is referred to as the α-c(4x4) structure.[18, 19] A third boron-induced reconstruction, the γ-(4x4) reconstruction, can also be formed, but is not shown here. It is important

to note that the presence of these boron-induced reconstructions indicates that the boron reacts very heterogeneously with the Si(001) surface, forming regions of high boron concentration separated by large regions of clean silicon. Many small patches of these boron-induced reconstructions can be found on the flat terraces and forming island structures on the large terraces; additionally, many small regions are formed near step edges (as in fig. 2c).

As the boron coverage is increased further, the number of boron-induced "A" and "B" features continues to increase. Fig. 3 shows a Si(001) surface exposed to 1000 Langmuirs B_2H_6 at 800 Kelvin, then followed with 90 seconds at 1000K. In this higher-coverage regime, the α-c(4x4) reconstruction, consisting of one "A" subunit and one "B" subunit in each unit cell, is the primary boron-induced feature. As at lower coverage, the boron-induced reconstructions segregate into large reconstructed regions, separated by regions of nearly-clean Si. In fig. 3, monatomic steps separate the large regions of clean Si near center and at left from the large boron-reconstructed regions; however, small islands of clean Si (labeled "Si") can be observed in the midst of the boron-reconstructed terrace.

In order to more fully understand the interaction of boron with Si(001), we have conducted two types of additional study. Through a detailed study of the boron-induced reconstructions using STM, in conjunction with other surface analysis techniques, we have developed a model for the boron-induced reconstructions. In addition, because of the presence of several different boron-induced reconstructions, we have also studied the ordering as a function of exposure rate, temperature, and other experimental variables.

Atomic structure of boron-induced reconstructions on Si(001)

In our previous work, we studied in detail the atomic-scale structure of the α-c(4x4), β-c(4x4), and γ-(4x4) reconstructions induced by boron on Si(001). Through quantitative measurements of boron and Si peak intensities in Auger electron spectroscopy, we determined that the reconstructed regions contained 1/2 monolayer of boron, in agreement with previous studies of "delta-doped" boron layers from other experimental groups using decaborane[15] and HBO_2 [6-8] as precursors. In addition, tunneling spectroscopy measurements showed that the "A" features have a high electronic state density just below E_F, and measurements of the surface photovoltaic effect show that the near-surface region becomes increasingly p-type as the boron coverage is increased. These last two measurements indicate that the boron atoms are electrically active p-type dopants, and suggest that the boron atoms are located on substitutional sites.

Based on the atomic-resolution STM measurements revealing the symmetry and location of the "A" and "B" features with respect to the underlying Si(001) lattice, analysis of the images as a function of coverage, and measurements of the changes in appearance as a function of applied bias, we have developed a structural model for the B-induced reconstructions on Si(001). As shown in fig. 4, in our model we attribute the "A" features to clusters of four boron atoms substitutionally located in the first full atomic layer. Because the "B"

features have the same symmetry as dimers of clean silicon, and because their appearance as a function of applied bias also tracks the changes observed for the clean Si surface, we attribute the "B" features to Si=Si dimers at the locations shown in this figure. Based on this model, all three boron-induced surface reconstructions can be attributed to combinations of the "A" subunit. Ordering of the "A" subunits alone produces the β-c(4x4) reconstruction, capping the A" subunits with Si=Si dimers produces the α-c(4x4) reconstruction, while capping half the A" subunits with Si=Si dimers produces a third boron-induced reconstruction, the γ-(4x4) reconstruction, which is found infrequently and not shown here.

While the details of this atomistic model for the boron-induced reconstructions is not central to this publication, it is important to recognize that all the experimental evidence as a function of coverage suggests that the boron-induced reconstructions arise from simple structural subunits. In particular, we note that the atomic structure of disordered or poorly-ordered regions can always be analyzed in terms of "A" and "B" structural subunits.

Ordering of Boron-induced Surface Reconstructions on Si(001)

Our STM measurements show that the primary boron-induced surface reconstructions on Si(001) have c(4x4) symmetry. Previous studies of boron "delta-doping" using HBO_2 as the precursor (but with otherwise identical annealing conditions) using electron diffraction have generally reported (2X1) structures,[6,7] although Sardela, et al. reported a (2X2) structure from elemental boron at lower coverage and higher sample temperature.[4] This discrepancy can be directly attributed to the spatial extent of the ordering. The individual ordered regions typically extend only 15-25 Å before being interrupted by a boundary with a different domain or one of the other reconstructions. Since the electron coherence length is typically on the order of 100 Å, this results in destructive interference between the different domains, leaving only the (2x1) Fourier components visible in most diffraction experiments

In order to investigate the surface ordering in more detail, experiments were conducted in which the temperature history of the sample was changed. Figure 5a shows a Si(001) surface after exposure to 3000L B_2H_6 at 800K. On distance scales of several thousand Ångstroms, fig. 5a shows that the surface remains comparatively smooth; however, the step edges no longer alternate between straight and wavy as the clean Si(001) surface does. The terraces contain larger regions which appear like "pits", which are one atomic layer deeper than the surrounding regions; in fig. 5a these pits occupy 23% of the total area. At high resolution, fig. 5b shows that the surface has the same structural features noted above at much lower coverage. In particular, the surface consists of ordered regions of α-c(4x4) and β-c(4x4) symmetry as described above, with a high concentration of domain boundaries between these structures. Thus, the surface shows clear ordering on distance scales of 10-15 Å, but is disordered on longer length scales.

We have found that ordering of the boron-induced reconstructions can be substantially improved if the exposure at 800 Kelvin is subsequently followed by a brief post-anneal in UHV at a higher temperature. Figure 6 shows that same sample as fig. 5, but now after an additional post-anneal at 1000 Kelvin for 90 seconds. On large distance scales, fig. 6a shows that the boron-reconstructed regions show substantially improved ordering, with reconstructed regions separated by larger regions of clean Si(001)-(2x1), labeled "Si". High-resolution STM images of the boron-reconstructed regions, as in fig. 6b, show that the post-annealing procedure substantially increases the ordering and results almost exclusively in the α-c(4x4) reconstruction. We further note that statistical analysis of the images indicates this the number of "A" features is unchanged by the post-anneal, so that little or no boron diffuses from the surface to the bulk during this process.

The post-annealing process is similarly effective at lower boron exposures. Fig. 7 shows an STM image obtained after exposure to 1000 Langmuirs diborane at 800 Kelvin followed by a post-anneal at 1000 Kelvin for 90 seconds. As at higher coverage, the post-annealing process produces a surface with good short-range order, and high-resolution images (fig. 7b) show that the surface consists primarily of segregated regions showing the α-c(4x4) boron-induced reconstruction, separated by regions of clean Si(001)-(2x1). In fig. 7a, we note that the c(4x4) reconstruction is observed both on the island structures as well as on the terrace. Because the c(4x4) reconstruction has an average apparent height which is lower than that of the clean Si(001) surface, large terraces exhibiting both the Si(001)-(2x1) reconstruction and the boron-induced α-c(4x4) reconstruction have a "patchy" appearance. This "patchiness" can be observed clearly in fig. 7 and fig. 5. In addition, however, even surfaces which are exposed to diborane at much lower exposures and/or temperature, as in fig. 1-2, show dark regions on the large flat terraces. In most cases, these dark regions arise from small regions (sometimes as small as 1-2 unit cells) of the boron-induced reconstructions which form in the large flat terraces rather than as island structures.

Although diffusion of the boron into the bulk will also occur under high temperature conditions,[15, 25] our experiments show that the long-range order can be substantially improved, without significant boron diffusion into the bulk, if the samples prepared as described above are subsequently annealed for short times at approximately 1000 Kelvin.

Comparison of Diborane and Decaborane as Precursors

Because diborane has a very low sticking coefficient on silicon even at 800 Kelvin, creating the boron-induced reconstructions shown in fig. 1-5 requires rather high exposures. In contrast, the molecule decaborane, $B_{10}H_{14}$, has a very high sticking coefficient. In order to confirm that the features described above can be attributed to the boron, we also conducted experiments using decaborane as a molecular precursor. Fig. 8 shows the Si(001) surface after exposure to 0.2 Langmuir $B_{10}H_{14}$ at 800 Kelvin. Most of the surface features appear identical to those observed with decaborane exposure, demonstrating

that the boron-induced reconstructions are not unique to using diborane as a precursor. In addition to the "A" and "B" subunits, however, fig. 8 also shows some individual protrusions which appear to be just half of the "A" subunits. These new features are labeled "A/2". These "A/2" units bridge-bonds between two dimers within in a single row, and have identically the same height and local symmetry as the individual protrusions within the "A" subunits described above. We also note that such "A/2" features are also observed in experiments with diborane at low temperature (740 K). Based on detailed experiments as a function of coverage and temperature, we conclude that these "A/2" features are indeed just one-half of the "A" subunit. The "A/2" features are observed only under conditions of low temperature, where limited mobility of the boron atoms likely prevents the accumulation of "A/2" subunits into the larger "A" subunits.

From such comparisons of B_2H_6 and $B_{10}H_{14}$, we reach two primary conclusions. The first is that the boron-induced structural rearrangements are observed for more than one molecular precursor, verifying that they indeed can be attributed to boron atoms in some structural form. Secondly, we note that the ordering produced by decaborane is less ideal than that produced by diborane exposure; this suggests that decaborane reacts homogeneously on the surface but boron atoms must diffuse together to form the ordered arrangements; in contrast, diborane reacts heterogeneously, such that the boron atoms have shorter distances to diffuse in order to form the ordered reconstructions. Further investigations into the detailed kinetics of boron ordering on Si(001) will be needed to completely understand differences between various molecular precursors.

Conclusions

In conclusion, we have studied the formation of the order structures for boron on Si(001) using STM and other surface analytical techniques. Our results demonstrate that the interaction of boron with Si(001) produces several different reconstructions, which arise from combinations of simpler building blocks. The net result is that there is a striking inhomogeneity in the distribution of boron across the surface, even at extremely low boron coverage. This spatial inhomogeneity has significant implications for the fabrication of nanometer-sized electronic devices, since it suggests that the local doping level will exhibit strong fluctuations resulting from this spatial variation. At high coverage, the ordering of boron to form an electrically-active sheet of charge permits the local concentration to exceed the bulk solubility limit with precipitating elemental boron. Such kinetically-stable structures provide an alternative means for controlling the properties of electronic devices in which the random statistics of conventional growth methods is replaced instead with atomic-level control.

Acknowledgment

This work is supported by the U.S. Office of Naval Research.

References:

[1] M.L. Yu, D.J. Vitkavage and B.S. Meyerson, J. Appl. Phys. **59**, 4032 (1986).

[2] B.S. Meyerson, F.K. LeGoues, T.N. Nguyen and D.L. Harame, Appl. Phys. Lett. **50**, 113 (1987).

[3] C.P. Parry, S.M. Newstead, R.D. Barlow, P. Augustus, R.A. Kubiak, M.G. Dowswtt, T.E. Whall and E.H.C. Parker, Appl. Phys. Lett. **58**, 481 (1991).

[4] M.R. Sardela, W.-X. Ni, J.O. Ekberg, J.-E. Sundgren and G.V. Hansson, Mat. Res. Soc. Symp. Proc. **220**, 109 (1991).

[5] T.L. Lin, R.W. Fathauer and P.J. Grunthaner, Appl. Phys. Lett. **55**, 795 (1989).

[6] R.L. Headrick, B.E. Weir, A.F.J. Levi, D.J. Eaglesham and L.C. Feldman, Appl. Phys. Lett. **57**, 2779 (1990).

[7] R.L. Headrick, B.E. Weir, A.F.J. Levi, B. Freer, J. Bevk and L.C. Feldman, J. Vac. Sci. Technol. A **9**, 2269 (1991).

[8] R.L. Headrick, B.E. Weir, A.F.J. Levi, D.J. Eaglesham and L.C. Feldman, J. Crystal Growth **111**, 838 (1991).

[9] B.E. Weir, R.L. Headrick, Q. Shen, L.C. Feldman, M.S. Hybertsen, M. Needels, M. Schluter and T.R. Hart, Phys. Rev. B **46**, 12861 (1992).

[10] B.E. Weir, L.C. Feldman, D. Monroe, H.-J. Grossmann, R.L. Headrick and T.R. Hart, Appl. Phys. Lett. **65**, 737 (1994).

[11] F. Eversteyn and B.H. Put, J. Electrochem. Soc. **120**, 106 (1973).

[12] T.Y. Hsieh, K.H. Jung, D.L. Kwong, Y.M. Kim and R. Brennan, Appl. Phys. Lett. **61**, 474 (1992).

[13] D.W. Greve and M. Racanelli, J. Electronic Materials **21**, 593 (1992).

[14] H.-C. Lin, H.-Y. Lin, C.-Y. Chang, T.-G. Jung, P.J. Wang, R.-C. Deng and J. Lin, J. Appl. Phys. **76**, 1572 (1994).

[15] D.D. Koleske, S.M. Gates and D.B. Beach, J. Appl. Phys. **72**, 4073 (1992).

[16] P. Avouris, I.W. Lyo, F. Bozso and E. Kaxiras, J. Vac. Sci. Technol. A **8**, 3406 (1990).

[17] P. Bedrossian, R.D. Meade, K. Mortensen, D.M. Chen, J.A. Golovchenko and D. Vanderbilt, Phys. Rev. Lett. **63**, 1257 (1989).

[18] Y. Wang, E. Frank and R.J. Hamers, Appl. Phys. Lett. **(submitted)**, (1994).

[19] Y. Wang, R.J. Hamers and E. Kaxiras, Phys. Rev. Lett. **(Submitted)**, (1994).

[20] X. Chen, B. Cousins, M. McEllistrem and R.J. Hamers, Rev. Sci. Instrum. **63**, 4308 (1992).

[21] R.J. Hamers, R.M. Tromp and J.E. Demuth, Phys. Rev. B **34**, 5343 (1986).

[22] I. Shapiro, C.O. Wilson, J.F. Ditter and W.J. Lehmann. in *Borax to Boranes, Advances in Chemistry Series* (eds. Gould, R.F.) 129 (American Chemical Society, Washington, D.C., 1961).

[23] K. Sinniah, M.G. Sherman, L. Lewis, W.H. Weinberg, J.T.J. Yates and K.C. Janda, J. Chem. Phys. **92**, 5700 (1990).

[24] Y. Wang, M.J. Bronikowski and R.J. Hamers, Surf. Sci. **311**, 64 (1994).

[25] H.-J. Gossmann and E.F. Schubert, Critical Rev. in Solid state and Materials Sci. **18**, 1 (1993).

Figure captions:

Fig. 1: STM images of Si(001) surface after exposure to 125L diborane at 800K.
a). Large area image, dimension: 418 Å x 363 Å, V_{sample} = - 1.8 V, I_{tunnel} = 0.3 nA;
b). High resolution image, dimension: 233 Å x 141 Å, V_{sample} = - 2.4 V, I_{tunnel} = 0.3 nA;
c). Height profile across the line shown in b). The inset shows the local symmetry of the "A" feature with respect to the underlying Si(001) lattice.

Fig. 2: STM image of Si(001) surface after exposure to 375L diborane at 800K, showing the formation of ordered structures. The three images reveal different aspect of the ordering as described in text.

a). Dimension: 146 Å x 146 Å, V_{sample} = - 2.3 V, I_{tunnel} = 0.3 nA;
b). Dimension: 100 Å x 100 Å, V_{sample} = - 2.3 V, I_{tunnel} = 0.3 nA;
c). Dimension: 178 Å x 154 Å, V_{sample} = - 2.0 V, I_{tunnel} = 0.3 nA.

Fig. 3: High-resolution STM image of Si(001) surface after exposure to 1000L diborane at 800K, followed by a post-anneal at 1000 K for 90 seconds. Dimension: 280 Å x 280 Å; V_{sample} = -1.9 V; I_{tunnel} = 0.2 nA.

Fig. 4: Proposed model for the "A" and "B" structural subunits and the arrangements of these subunits to form the α-c(4x4), β-c(4x4), and γ-(4x4) unit cells of the boron-induced reconstructions of Si(001).

Fig. 5: a). STM image of Si(001) surface after exposure to 3000L diborane at 800K showing the overall surface morphology. Dimension: 2530 Å x 2530 Å, V_{sample} = -2.0 V; I_{tunnel} = 0.1 nA;
b). High resolution image prepared as in (a), revealing partial ordering of the boron-induced features. Image dimension: 133 Å x108 Å, V_{sample} = -2.6 V; I_{tunnel} = 0.3 nA;

Fig. 6: STM images taken after exposure of Si(001) to 3000L B_2H_6 at 800K, followed by annealing at 1000K for 90 seconds.
a). Large scale image showing nearly complete coverage with boron-induced reconstructions and less than 15% remaining as "clean" Si(001)-(2X1). Dimension: 890 Å x 890 Å, V_{sample} = -2.0 V, I_{tunnel} = 0.3 nA,
b). High resolution image show nearly perfect c(4X4) ordering from the ordered arrangement of "A" and "B" features. Dimension: 86 Å x 67 Å, V_{sample} = -2.0 V; I_{tunnel} = 0.3 nA.

Fig. 7: STM images show the effect of post-annealing on the surface order. Images were obtained after exposing Si(001) surface to 1000L B_2H_6 at 800K, then annealing at 1000K for 90 seconds.
a). Large scale image showing coexisting reconstructed islands and substrates, dimension: 1200 Å x 1010 Å, V_{sample} = -1.6 V; I_{tunnel} = 0.3 nA;
b). Higher-resolution image showing that the composition and structure are the same for both island and reconstructed substrate, dimension: 243 Å x 258 Å, V_{sample} = -1.9 V; I_{tunnel} = 0.2 nA.

Fig. 8: STM image of Si(001) surface after exposed to 0.2 L $B_{10}H_{14}$ at 800K including the "A/2" feature. Dimension: 244 Å x 340 Å, V_{sample} = -1.6 V, I_{tunnel} = 0.2 nA.

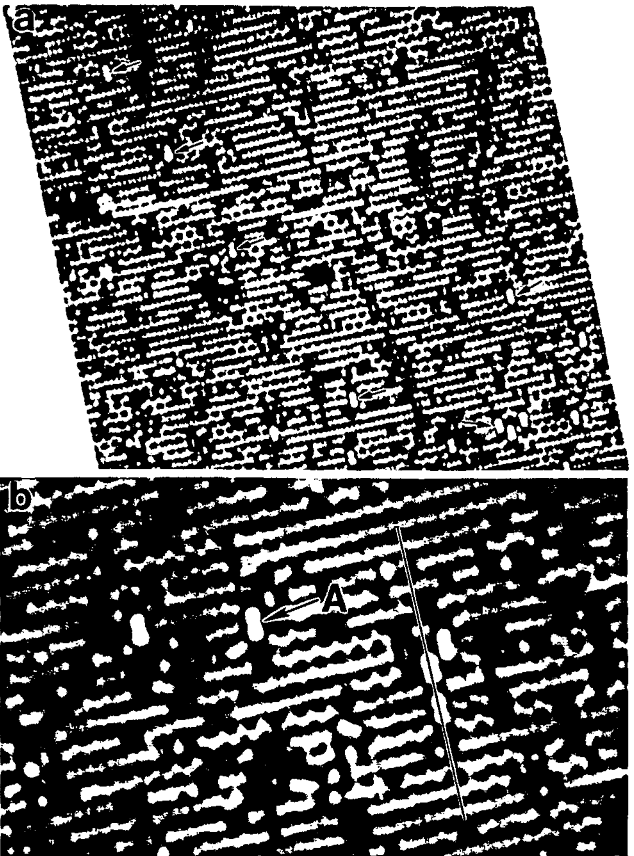

Wang and Hamers
J. V. S. T.
Figure 1

Wang and Hamers
J. V. S. T.
Figure 2

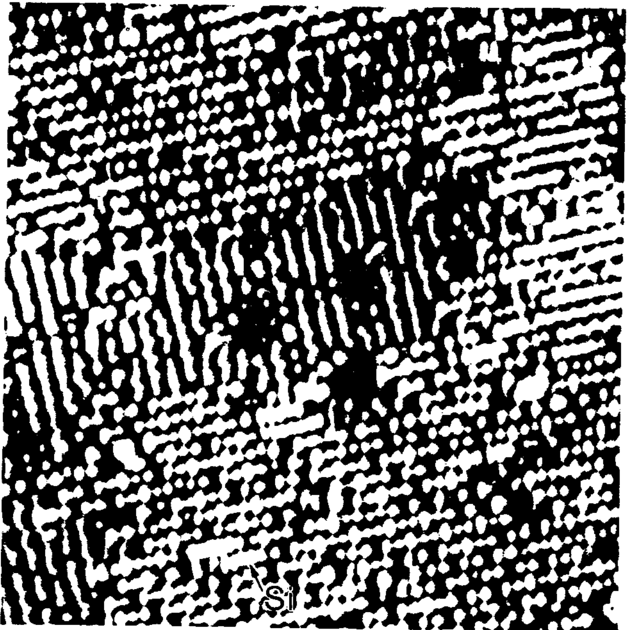

Wang and Hamers
J. V. S. T.
Figure 3

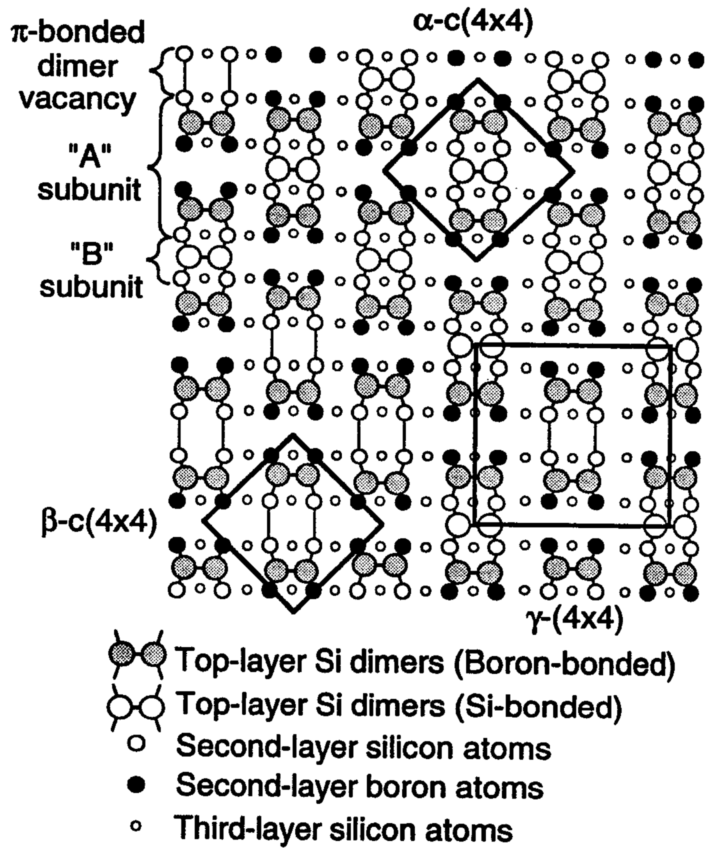

Wang and Hamers
J. V. S. T.
Figure 4

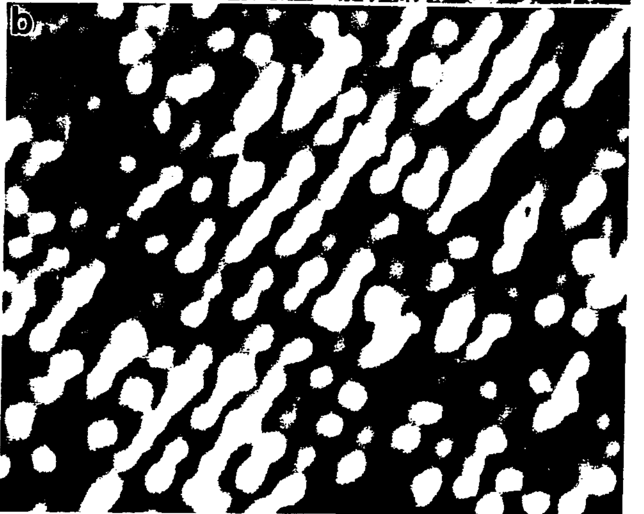

Wang and Hamers
J. V. S. T.
Figure 5

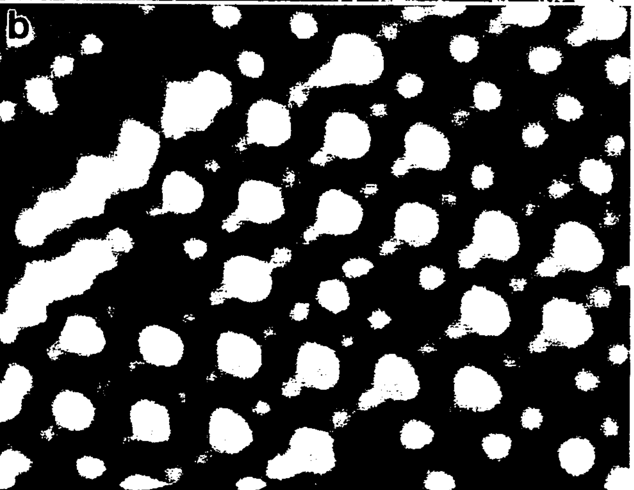

Wang and Hamers
J. V. S. T.
Figure 6

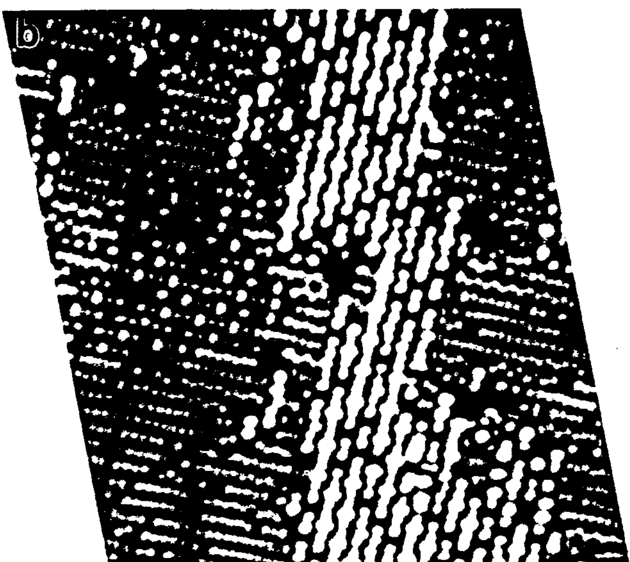

Wang and Hamers
J. V. S. T.
Figure 7

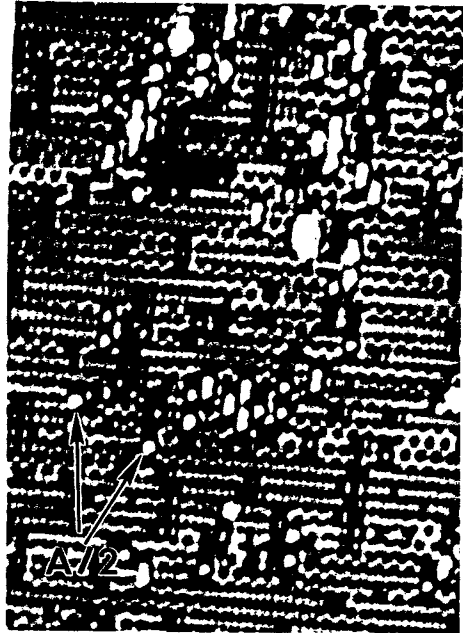

Wang and Hamers
J. V. S. T.
Figure 8